

〈論 文〉

## 얕은 감세지내의 세굴능 분포형태의 예측 Prediction of Scour Potential Distributions in a Shallow Plunge Pool

손 광 익\*  
SON Kwang Ik

**Abstract**□ Because a failure to provide enough plunge pool depth can create a risk to the structural stability of the spillways or dams, many researchers have proposed experimental formulas for calculating ultimate scour depth under jet issued from spillways and pipe culverts. For the design purposes of a plunge pool, scour potential distribution is important as much as the ultimate scour depth is. In this study scour potential distributions near the jet impinging point on a porous plane which can simulate a real cohesionless movable flat bed has been measured. Experimental results showed that scour potential distributions are geometrically similar to each other provided the angle of jet impact was the same. Statistical analysis of experimental results showed that scour potential distributions for the design purposes of a plunge pool could be expressed by a single equation within a range of this experiment. The proposed formula for the prediction of scour potential distributions agrees well with experimental measurements.

**요 지 :** 여수로 하류부의 감세지내 세굴이 설계 기준치 이상으로 진전될 경우 여수로나 댐의 구조적 안정성을 위협하게 되는 심각한 상황이 야기되므로 감세지내의 극한 세굴깊이 예측에 대한 많은 연구들이 이루어져 왔으나 감세지의 설계에 필수적인 세굴능의 분포특성에 대한 연구는 거의 이루어지지 않았다. 따라서 본 연구에서는 여수로나 관거로 부터 방류되는 켈이 비점착성 하상에 도달되는 원형의 이상적인 모델을 개발하여 감세지 하상에서의 세굴능 분포를 측정하였다. 실험 연구결과 동일한 켈 입사각의 경우 세굴분포는 켈의 수리학적특성이나 감세지 깊이에 관계없이 실험 범위내에서는 기하학적으로 유사하다는 사실과 감세지의 설계목적만을 위한 세굴능의 분포형태는 켈의 입사각에 관계없이 실험 범위 내에서는 하나의 식으로 표현될 수 있다는 사실을 통계학적 분석을 통하여 알아내었다. 또한 유도된 세굴분포식을 이용한 결과 실측치와 잘 일치됨을 확인하였다.

### Introduction

Many researches of the flow characteristics of jet impinging on a flat plane have been carried out in the heat transfer field and in the aerodynamic field. Even though studies about jet impingement on a flat surface provide good insights on impingements of a jet, a common problem of these researches is that

the experiments were performed with smooth flat bed. This boundary condition differs to the bed boundary conditions of a real plunge pool. It is also clear that the effect of bed surface roughness and the porosity of bed boundary can not be ignored. Engineers often encounter hydraulic structures which do not allow a deep tailwater depth. Therefore, studies of the scour potential distribution were carried out to aid the design of plunge pool

\* 정희원, 영남대학교 토목공학과 전임 강사

bed with shallow tailwater depth under jet issued from spillways and pipe culverts.

### Literature Review

Schauer and Eustis(1963), Kamoi and Tanaka(1972), and Beltaos(1976) measured flow characteristics of two dimensional jet impinging on a flat surface. Beltaos(1974) systematically studied flow properties with rectangular and circular jet at different impingement angles. Beltaos and Rajaratnam (1974) found that velocity profiles were similar for  $l/H$  less than 0.95 and that static pressure distributions of the impingement region were similar.  $l/H$  is the ratio of jet travel length to the distance between jet exit and bed surface. Beltaos(1974) derived dimensionless wall shear stress for inclined jet. Kamoi and Tanaka(1972) measured shear stress with hot film probes and found that distribution of wall shear stress on a plane had two peaks near the stagnation point depending upon the angle and height of impingement. Wu and Rajaratnam(1990) discussed the effects of boundary roughness and characteristics of a circular turbulent wall jet growing on a rough boundary.

### Experiments

Dimensional analysis is applied to find the dimensionless parameters which influence scour. The experiments were performed with a circular submerged jet in a rectangular channel. Taraimovich(1978) found that jet impact angle usually ranged from  $25^\circ$  to  $46^\circ$  for wide lower plunge pool ( $4 \leq$  the ratio of river width to tailwater depth  $\leq 75$ ). Therefore, this study was performed with the angle of jet impact  $28.5^\circ$  and  $45^\circ$ . An idealized

model of jet impinging into cohesionless porous flat bed was proposed by Son et al. (1993). The significant variables used in their model are shown in Fig. 1. The adopted significant variables were nozzle diameter( $D_n$ ), average flow velocity at nozzle ( $U_o$ ), angle of jet impact on tailwater surface( $\theta$ ), width of plunge pool ( $B$ ), tailwater depth ( $H$ ), density of water( $\rho$ ), kinematic viscosity of water( $\nu$ ), diameter of bed material( $D_s$ ) and the submerged sphere weight ( $W_s = (\rho_s - \rho)g\pi D_s^3/6$ ).

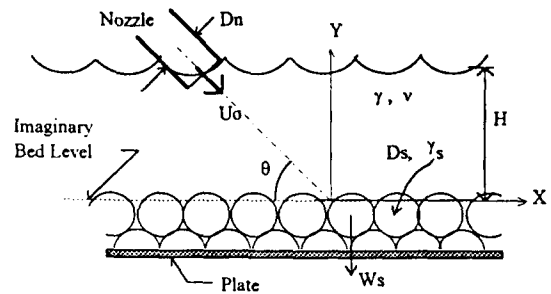


Figure 1. Schematic diagram of experiments

By selecting  $D_n$ ,  $\rho$  and  $U_o$  as the repeating variables, Son et al.(1993) developed the following dimensionless terms.

$$\frac{\rho_s - \rho}{\rho} \frac{g D_s^3}{U_o^2 D_n^2} = f_1(D_s/D_n, H/D_n, X/D_n, B/D_n, \nu/U_o D_n, \theta) \quad (1)$$

Son et al.(1993) found in their experimental works that Eq.(1) could be reduced as Eq.(2) or Eq.(3). They confirmed Albertson et al's (1950), Hartung and Hausler's (1973), and Maynord's (1988) studies that the effect of Reynolds number on the jet diffusion is negligible.

$$W_s/M_o = (\rho_s - \rho)gD_s^3/(\rho U_o^2 D_n^2) = f_2(D_n/D_s,$$

$$H/D_s, \theta \quad (2)$$

$$W_s/M_{os} = (\rho_s - \rho)gD_s / (\rho U_o^2) = f_3(D_n/D_s, H/D_s, \theta) \quad (3)$$

where,  $W_s$ ; submerged sphere weight =  $(\gamma_s - \gamma)\pi D_s^3/6$

$M_o$ ; jet momentum at nozzle exit =  $\rho\pi D_n^2 U_o^2/4$

$M_{os}$ ; jet momentum acting on a sphere =  $\rho\pi D_s^2 U_o^2/4$

Sixty-one experiments were carried out to measure  $W_s/M_o$  ( $W_s/M_o$  will be named "scour potential") for three nozzle diameters (2-inch, 3-inch and 4-inch), six tail water depths ( $H/D_n = 1.83-6.95$ ), and various Reynolds numbers. The experimental ranges are summarized in Table 1. The jet travel length of this research reaches up to 13.5 times the jet diameter. Hartung and Hausler(1973) found that most of jet energy dissipated at a distance of 20 time the jet diameter.

Table 1. Experimental Ranges of This Research

Description	Experimental Range
Jet Reynolds No.	80,000-222,000
Impact Angle of Jet on Plunge Pool Surface	28.5° -45°
The Ratio of Jet Diameter to Bed Material Diameter	0.8-1.6
The Ratio of Jet Diameter to Jet Travel Length	1.7-13.5

The next four figures (Fig. 2-5) are the examples of the experimental results for 45° and 28.5° of jet impact angle. For the jet impact angle 45°, a clear trough was found in the middle of scour potential distribution curve. Some experimental results of the jet impact angle 28.5° show slight trough. It seems that the trough occurs due to an effect of jet stagnation point on the plunge pool bed. A steep gradient of scour potential distribution near the stagnation point indicates there exist strong turbulences near the stagnation point.

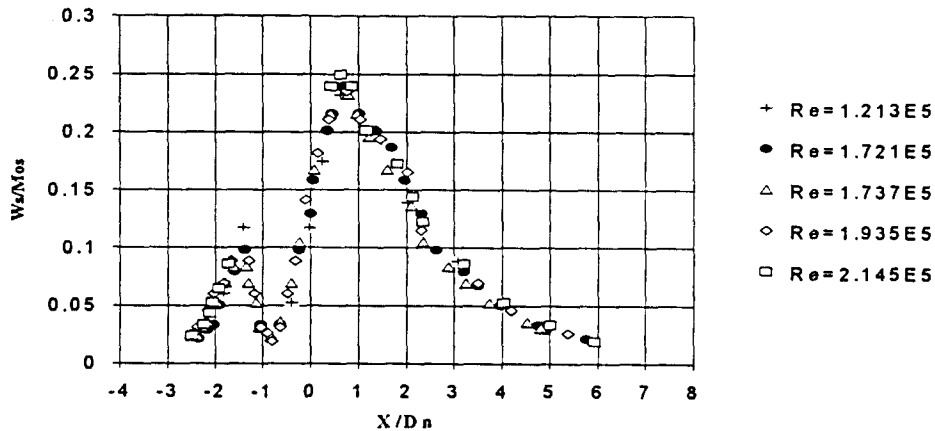


Figure 2. Scour potential for  $H/D_n=2.32$  (4-inch nozzle,  $\theta=45^\circ$ )

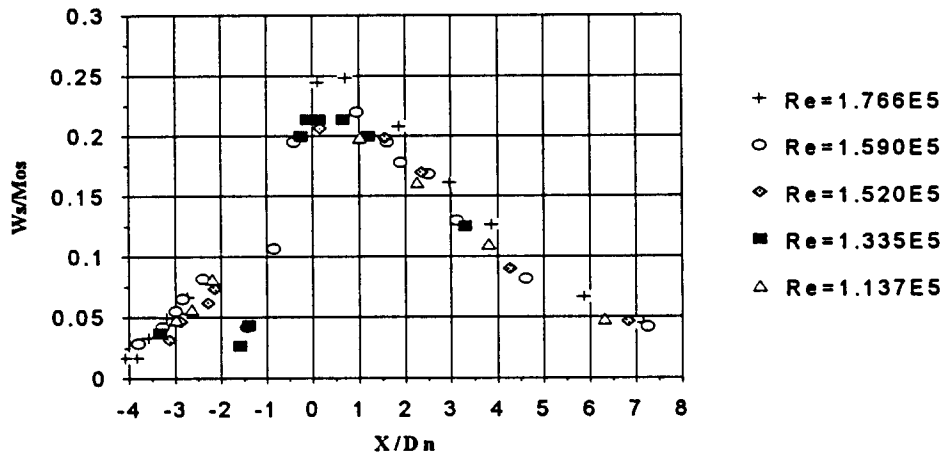


Figure 3. Scour potential for  $H/D_n=6.53$  (2-inch nozzle,  $\theta=45^\circ$ )

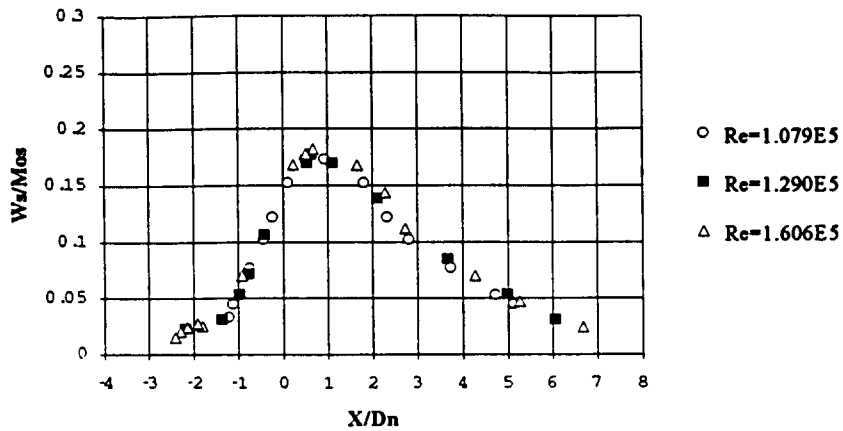


Figure 4. Scour potential for  $H/D_n=2.60$  (4-inch nozzle,  $\theta=28.5^\circ$ )

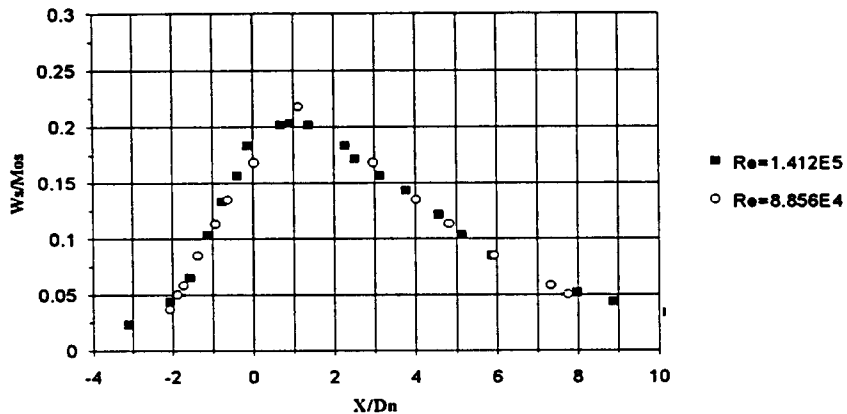


Figure 5. Scour potential for  $H/D_n=5.24$  (2-inch nozzle,  $\theta=28.5^\circ$ )

### Analysis of Experimental Results

Fig.2 through Fig.5 show that the patterns of scour potential distributions are very similar for the same angle of jet impact. Therefore, an attempt was made to see if there exists a geometrical similarity among the scour potential distribution curves for each angle of jet impact.

At first, the measured scour potentials were normalized by their max.  $W_s/M_{os}$ . The normalization result for  $\theta=45^\circ$  is shown in Fig.6.

Each distribution was moved by  $L_c$  in negative horizontal direction so the apex of normalized scour potential curve passes  $X/D_n=0$  and the normalized  $W_s/M_{os}=1$ . In Fig. 6, larger  $H/D_n$  shows the larger dispersed tail width of the scour potential curve. The scattered tail parts of the distributions could be collapsed into a line by dividing the  $(X/D_n - L_c)$  with scaling factor ( $S_c$ ). The scaling factor ( $S_c$ ) was adopted by measuring the dispersed tail width of the distribution curve

along the horizontal line crossing 0.5 of the normalized  $W_s/M_{os}$ .

The results of normalizing, centering, and scaling of the data are shown in Fig. 7 and Fig. 8. The figures show that there exists a unique scour potential pattern for each angle of jet impact, i.e., there exists a geometrical similarity among the scour potential distributions for each angle of jet impact. Statistical analysis showed that scaling factor ( $S_c$ ) and centering magnitudes ( $L_c$ ) could be expressed as follows with correlation coefficients squared ( $r^2$ ) equal 0.94 and 0.67, respectively.

$$S_c = 1.75 - 2.57\theta + 2.27D_n/D_s + 1.10H/D_n - 1.50(D_n/D_s)(H/D_n) + 0.631(H/D_n)Re + 1.30\theta(D_n/D_s)(H/D_n) - 0.842\theta(H/D_n)Re \quad (4)$$

$$L_c = 0.337 - 0.0304H/D_n + 0.399\theta(D_n/D_s) \quad (5)$$

For design engineers in civil engineering practices, a simplified scour potential distribution shape for any jet impact angles ( $28.5^\circ - 45^\circ$ ) will be convenient. The suggested simple curve shape is shown in Fig. 9.

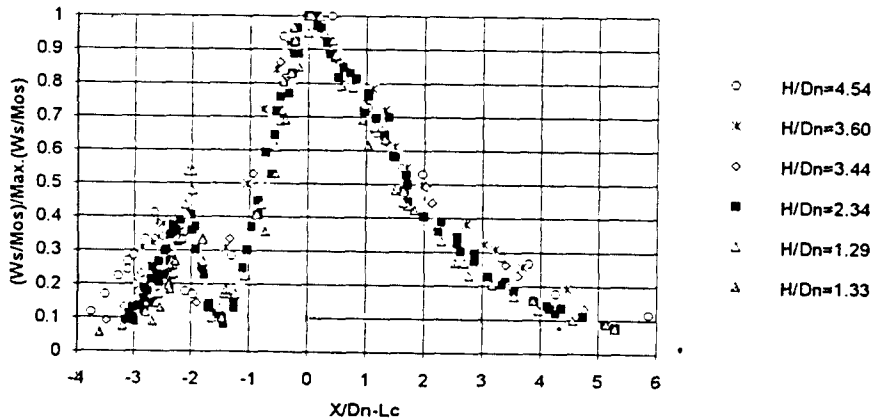


Figure 6. Normalized Scour Potential Distribution for  $\theta=45^\circ$

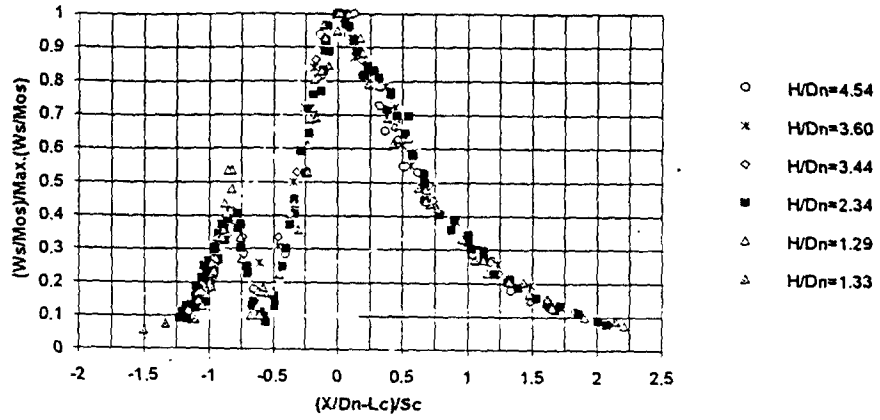


Figure 7. Unified scour potential distribution for  $\theta=45^\circ$

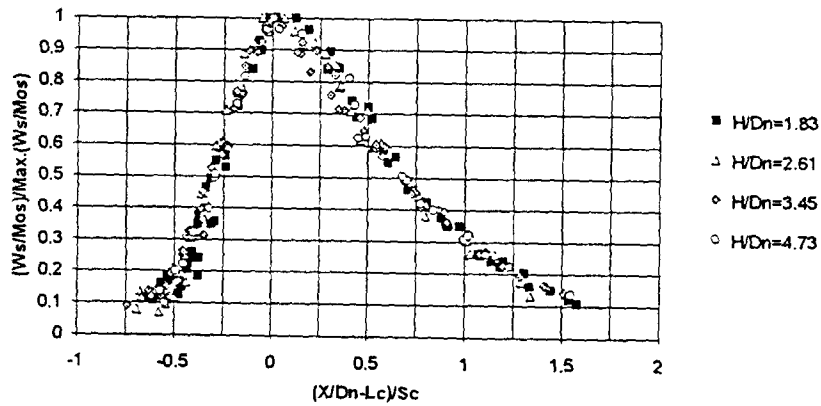


Figure 8. Unified scour potential distribution for  $\theta=28.5^\circ$

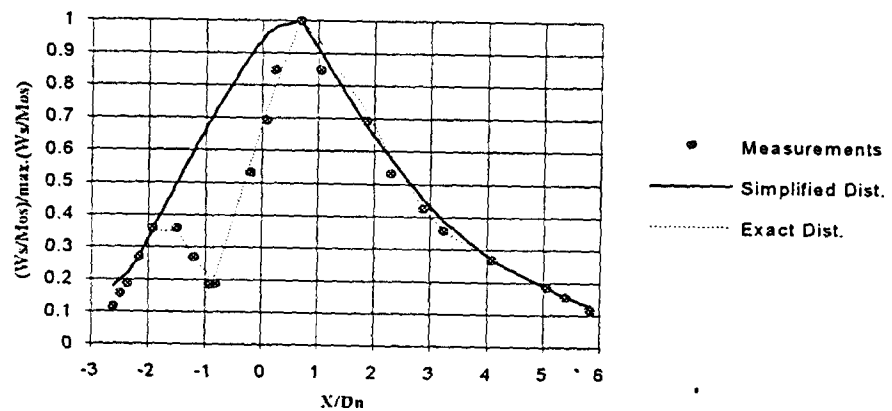


Figure 9. Simplified and Exact Scour Potential Distribution Curves

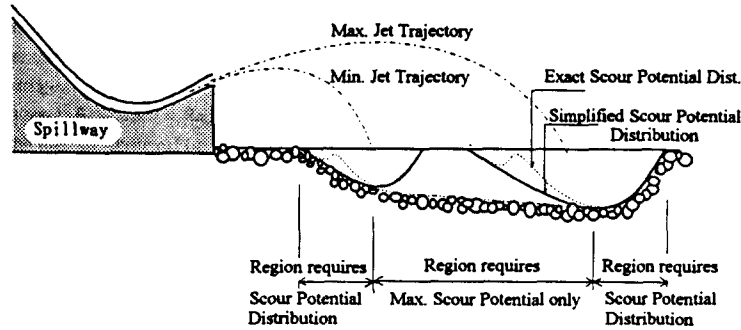


Figure 10. Explanation of Two Regions within Scour Hole

Because the point where the maximum scour depth occurs is varying during the operation of spillways, the plunge pool design does not require an exact score potential distribution except at the edges of scour hole. As shown in Fig. 10, two regions of scour hole should be considered to predict the scour hole shape. One is a region where maximum scour potential governs a scour hole shape. Another is a region where maximum scour potential and scour potential distribution govern a scour hole shape. Fig. 10 illustrates which parameters should be considered in predicting a scour hole shape.

Weibull, Gaussian, revised Type 1, Type 2 and Type 3 distribution curves (Benjamin and Cornell, 1970) were applied in regression analysis to find optimally simplified scour potential distribution curve. Statistical analysis showed that the revised Type 1 distribution has the highest correlation with normalized scour potential distribution regardless of the angle of jet impact. The average correlation coefficient squared ( $r^2$ ) of 61 regressions is 0.9794.

$$\frac{(W_s/M_{os})}{\text{Max.}(W_s/M_{os})} = m_3 m_1 \exp [-m_1 (X/D_n - m_2) - \exp(-m_1(X/D_n - m_2))] \quad (6)$$

The results of multiple regression analysis are

$$\ln(m_1) = 0.0816 + H(-0.381 + 0.277 + 0.308D) + D(-0.186 - 0.358Re - 0.338 \theta H) + 0.452 \theta Re \quad (7)$$

$$m_2 = 1.22 + D(0.892 - 0.209H) + 0.244 H + \theta(-3.05 - 0.378 D Re + 0.695 Re) \quad (8)$$

$$m_3 = 0.924 + 2.95D - 1.68 \theta D Re + 0.648 Re^2 + H\{1.39 + \theta(-1.24 + 2.16D - 0.6Re) - 1.83D + 0.364Re + 0.0570 H\} \quad (9)$$

where,  $m_1, m_2, m_3, ;$  the coefficients of Eq. (6)

$D$  : ratio of nozzle size to gravel size ( $D_n/D_s$ )

$H$  : ratio of pool depth to nozzle size ( $H/D_n$ )

$Re$  : Reynolds number at nozzle exit divided by  $1.0 \times 10^5$ .

### Comparisons and Conclusions

Actual scour potential distribution can be calculated by multiplication of the maximum scour potential to Eq.(6). Son(1993) proposed

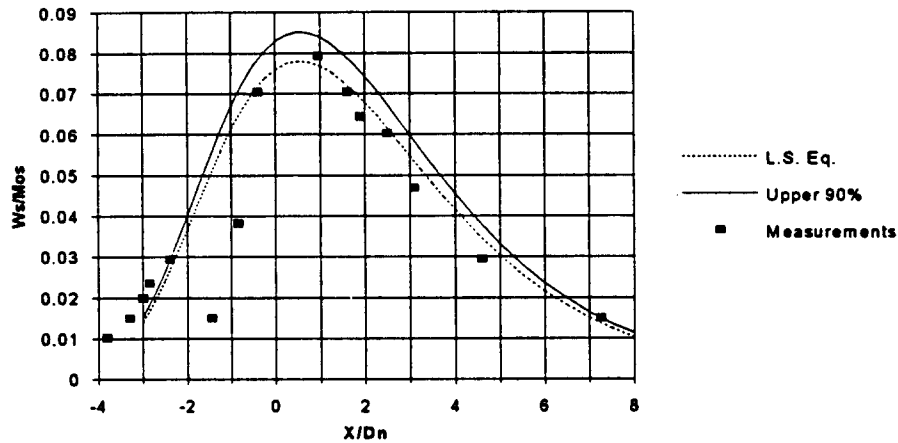


Figure 11. An Example of Estimated and Measured Scour Potential for  $\theta=45^\circ$   
(3-inch nozzle,  $H/D_n=4.443$ , and Reynolds No.  $=9.19 \times 10^4$ )

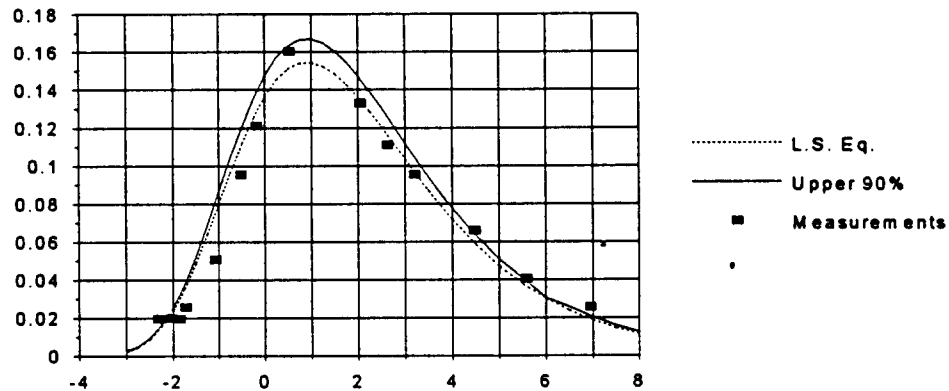


Figure 12. An Example of Estimated and Measured Scour Potential for  $\theta=28.5^\circ$   
(4-inch nozzle,  $H/D_n=3.45$ , and Reynolds No.  $=1.874 \times 10^5$ )

equations for the prediction of maximum scour potential. The next two figures (Fig. 11–Fig. 12) show the comparisons of raw experimental measurements of scour potential with predicted scour potential curves. “L.S. Eq.” in Fig. 11 and Fig. 12 stands for the least square equation. “Upper 90 percent” stands for the upper 90 percent prediction values of maximum scour potential. As shown in Figs. 11 and 12, developed formulas for the prediction of scour potential distribu-

tion agree with experimental measurements.

1. Regardless the flow characteristics of jet, scour potential distributions could be expressed with a single curve for the same angle of jet impact. In other words, the scour potential distributions are geometrically similar to each other if the angle of jet impact was the same.

2. The jet dispersion, magnitude of distribution and a point where the maximum scour



potential occurs depends upon tailwater depth and the ratio of jet size to the bed material size. The existence of jet stagnation point on the plunge pool bed was observed and strong turbulences near the stagnation point were found from experiments. A jet generates maximum scour potential downstream of the point where the extension of jet centerline intersects the bed level.

3. Within the experimental range (jet impact angle ;  $28.5^\circ$  and  $45^\circ$  ), the scour potential distributions for engineering design purposes could be expressed with a revised Type I distribution curve.

### References

1. Albertson, M.L., Y.B. Dai, R.A. Jesen, and H. Rouse (1952) Diffusion of submerged jets, Transactions of ASCE, Paper No.2409, pp.639-664
2. Beltaos, S., and N.Rajaratnam (1973) Plane turbulent impinging jets. IAHR, Journal of Hydraulic Research Vol.11, No.1, pp.29-59.
3. Beltaos, S., and N.Rajaratnam(1974) Impinging circular turbulent jets. ASCE, Journal of Hydraulics Div. Vol.100, No.HY10, pp.1313-1328.
4. Benjamin, J.R., and C.A.Cornell(1970) "Probability, Statistics, and Decision For Civil Engineers." McGraw-Hill Book Co., New York, 684p.
5. Kamoi, A., and H. Tanaka(1972) Measurements of wall shear stress, wall pressure and fluctuations if the stagnation region produced by oblique jet impingement. (Fluid Dynamic Measurements in the Industrial and Medical Environmental). Proceedings of the Disa conference held at the University of Leicester, Leicester University press. Vol.1, pp.217-227.
6. Maynard, S.T. (1988) Stable riprap size for open channel flows. Dept. of the Army, Wa-

- terways Experiment Station, COE, Vickburg, Mississippi, Technical Report HL-88-4. 115p.
7. Son, K.I.(1994) Prediction of ultimate scour potentials in a shallow plunge pool. The Journal of KAHS. Vol.27, No.1, pp.123-132
8. Son, K.I., W.Lee, and W.Cho(1993) Experimental analysis of the parameters governing scour in plunge pool with cohesionless bed material. Proceedings of the Korean Society of Civil Engineers, Vol.13, No.4, pp.123-130.
9. Taraimovich, I.I.(1978) Deformations of channels below high - head spillways. Hydrotechnical Construction, Vol.9, September, pp.917-923.
10. Wu, S., and N.Rajaratnam(1990) Circular turbulent wall jets on rough boundaries. IAHR, Journal of Hydraulic Research Vol.28, No.5, pp.581-589.

### NOTATIONS

The following symbols are used in this paper:

- B = Plunge pool width ;
- $D_n$  = Nozzle diameter ;
- $D_s$  = Sphere diameter ;
- H = Tailwater depth ;
- l = Travel length of jet ;
- $M_o$  = Total Momentum of jet at a nozzle exit ;
- $M_{os}$  = Momentum of jet acting on a projected area of sphere normal to jet direction ;
- $U_o$  = Velocity of jet at nozzle ;
- $W_s$  = Submerged weight of sphere ;
- X = Axis along bed level ;
- Y = Axis normal to bed level ;
- $\theta$  = Agle of jet impact (radian) ;
- $\nu$  = Kinematic viscosity of water ;
- $\rho$  = Density of water ; and
- $\rho_s$  = Density of bed material.